Available online at www.sciencedirect.com
SCIENCE DIRECT®
Electrochimica Acta 50 (2005) 4763–4770
ELECTROCHIMICA Acta
www.elsevier.com/locate/electacta

Synthesis, characterization and electrochemical properties of copper phosphide (Cu_3P) thick films prepared by solid-state reaction at low temperature: a probable anode for lithium ion batteries

Heriberto Pfeiffer [a,*], Franck Tancret [b], Thierry Brousse [b]

[a] *Instituto de Investigaciones en Materiales, Universidad Nacional Autónoma de México, Circuito exterior s/n, Ciudad Universitaria, Apdo. Postal 70-360, Coyoacan 04510, México D.F., Mexico*
[b] *Laboratoire de Génie des Matériaux, Ecole Polytechnique de l'Université de Nantes, BP50609, 44306 Nantes Cedex 3, France*

Received 20 January 2005; received in revised form 18 February 2005; accepted 18 February 2005
Available online 24 March 2005

Abstract

Copper phosphide (Cu_3P) was produced as thick films over copper foils. The synthesis was performed by solid-state reaction at low temperature (400 °C). Similar attempts were carried out for other transition metals of the first series without success. Scanning electron microscopy (SEM) revealed the formation mechanism of the Cu_3P thick films. First, phosphorus diffuses into the copper foil followed by the subsequent formation of the binary compound. During this process, the Cu_3P particles seem to dig the copper foil, producing holes, where the Cu_3P crystallites nucleate and growth. Then, the thick films are formed by the conjugation of several agglomerates and their morphology is not homogeneous. Oxidation of Cu_3P occurs to a small extend on the top surface of the films. The electrochemical behaviour of the thick film was compared with a standard Cu_3P composite electrode, in which the active material is mixed with carbon and a binder. Although the two different electrodes presented some differences in their electrochemical behaviour, both electrodes showed promising qualities to be used as anode materials in lithium ion batteries or hybrid devices.

Keywords: Copper phosphide; Lithium ion batteries; SEM; Solid-state reaction; Thick film

1. Introduction

Rechargeable Li ion batteries are key components for many equipments required in today's life. This kind of cells deliver almost 4 V, they have specific energies close to 120 Wh/kg and they have long shelf life at room temperature [1,2]. Nowadays, the study of lithium ion batteries is essentially divided into three fields, cathodes, anodes and electrolytes. Since 1970, graphite is the most commonly studied material as negative electrode and it is extensively used in commercial devices. Although in the last 10–15 years, several materials, such as metal oxides and intermetalics have been proposed as possible anode materials [3–5], most of these alternative anode materials fail to combine a high specific capacity, a low working potential and a high cyclability. The main reason is that most of the materials studied up to know lead to drastic structural changes when reacting with lithium, and subsequently, fail to retain their pristine electrochemical properties during long term cycling. Then, intensive research is carried out in that field. Hence, "new" materials are still proposed as alternative negative electrodes for lithium ion batteries.

Phosphorus forms solid compounds with nearly all the elements in the periodic table, but the phosphides are not as well known as many others compounds [6]. Nevertheless, in the last 5 years, several phosphides have been proposed as alternative anodes for lithium ion batteries [7–17]. These compounds seem to have high reversible capacities, and some of them good cyclability. The electrochemical reaction mech-

* Corresponding author. Tel.: +52 55 56224641; fax: +52 55 56161371.
E-mail address: pfeiffer@zinalco.iimatercu.unam.mx (H. Pfeiffer).

0013-4686/$ – see front matter © 2005 Elsevier Ltd. All rights reserved.
doi:10.1016/j.electacta.2005.02.024

anism, proposed for the metal phosphides versus lithium, depends on many factor such as, the structure of the material, the transition metal and the amount of lithium in the pristine compound. For example, in some cases, the pristine structure of the metal phosphide can be reversibly modified and reconstructed upon electrochemical cycling [9,12]. On the other hand, other phosphides are decomposed during the first cycles, and lithium reversible reacts with phosphorus to form Li_3P [10,11].

Apparently, metal phosphides may be an option as anodic materials. However, the synthesis of all these materials is usually complicated and requires the use of special devices, such as sealed tubes and they have to be handled and stored under inert atmospheres. All these special conditions prevent an easy industrial preparation. Copper phosphide (Cu_3P) presents good qualities as negative electrode. The gravimetric capacity of Cu_3P is close to that of graphite, but its volumetric capacity is almost four times higher than that of graphite [7,18]. This material is usually synthesized at high temperatures (800 °C). In a previous letter, we reported a new and very simple method to produce Cu_3P by solid-state reaction at low temperatures that could be easily scaled industrially [7]. We have presented how a thick film of Cu_3P can be produced over a Cu foil, and how this compound reversibly reacted with lithium. Then, the aim of the present work is to give more details about the synthesis of the Cu_3P films produced by this new method, and to show how large amounts of powder of this material can be produced in a very simple way. Finally, standard composite electrodes, with binder and conductive additives, were prepared with the powder produced by the Cu_3P thick films and electrochemically compared the thick films.

2. Experimental section

Cu_3P was synthesized by a new and very simple process, involving a solid-state reaction at low temperature [7]. Red phosphorous (99%, Aldrich) was suspended in ethanol. Then, the suspension was sprayed on a copper foil (Goodfellow, Cambridge Limited) previously heated in air at 60–70 °C. Once the ethanol was evaporated, a black–red brittle film was produced over the Cu foil. A set of these samples was fired at different temperatures for 8 h in flowing argon, producing in all cases a black thick film.

Different techniques were used to characterize the Cu_3P samples. Thermogravimetric analysis (TGA) and differential scanning calorimetry (DSC) were performed in a TA Instruments equipment. The heating rate used, for both techniques, was 5 °C/min from room temperature to 500 °C. All the measurements were performed in flowing N_2. X-ray diffraction (XRD) patterns were recorded with a Siemens D-5000 diffractometer, using the Cu Kα1 radiation. The particle size and morphology of the films were studied with a scanning electron microscope (SEM, LEO stereoscan 440) coupled with an energy dispersive X-ray analyzer (EDS, Link Isis, Oxford Instrument). Finally, the X-ray photoelectron spectra were recorded with a Leybold LHS12 system. The measurements were preformed using a Mg Kα anode (1253.6 eV) as the X-ray source, with an input power of 144 W. This system is equipped with a spherical capacitor analizer EEA 10 MCD, used in the fixed analysing mode and a twin channel plate detector split into 18 channels. The pressure in the analysis chamber was maintained in the low 10^{-7} Pa range during measurements. The pass energy was 50.4 eV. The elemental percentage analysis was calculated using the area under the XPS curves, divided by the atomic sensitivity factor for each element. An ablation process was applied to the samples into the XPS equipment. The conditions of the argon plasma for the ionic ablation process were 8 mA and 2.5 keV under a pressure of 3.5×10^2 Pa.

Concerning the electrochemical analysis, samples were tested in two different ways. Some samples were tested as they were prepared, as a thick film of Cu_3P over the copper substrate. On the other hand, other electrochemical tests were performed with Cu_3P composite electrodes. The composites were produced with Cu_3P powder scratched mechanically from the films. Afterwards, they were prepared as follows: Powder of Cu_3P, black carbon and TEFLON® as binder, were mixed in ethanol, using a molar ratio equal to 85:10:5, respectively. The electrochemical response of all the samples was tested on a Mac-Pile equipment (BioLogic), using a two-electrodes cell and metallic lithium as the counter electrode. The electrolyte used was 1 M solution of $LiPF_6$ in ethylene carbonate:diethyl carbonate (Merck), with a molar ratio of 1:2.

3. Results and discussion

3.1. Synthesis and composition of the Cu_3P thick films

Fig. 1A shows the TGA/DSC curves recorded for the Cu–P foil before any heat treatment. While the sample lost weight between room temperature and 200 °C, the sample presented an endothermic process in the same range of temperature. In this range of temperatures, the weight loss of the sample was not higher than 2%. This process is associated to evaporation of ethanol and possible dehydration of the red phosphorus precursor. This is in good agreement with the two different slopes observed on the endothermic part of the DSC curve, between 25 and 160 °C and between 170 and 230 °C. Each part of this endothermic process was attributed to the organic decomposition of the ethanol, and the dehydration, respectively. From 240 to 500 °C, the sample did not present any significant change of weight. However, the DSC curve shows two small endothermic peaks at 320 and 465 °C. The first peak, at 320 °C, can be due to the first stage of atomic movements and Cu_3P formation. On the opposite way, the second peak must be associated with an oxidation process of the Cu_3P. As we will demonstrate later in this paper, the Cu_3P thick film suffers oxidation over the top surface.

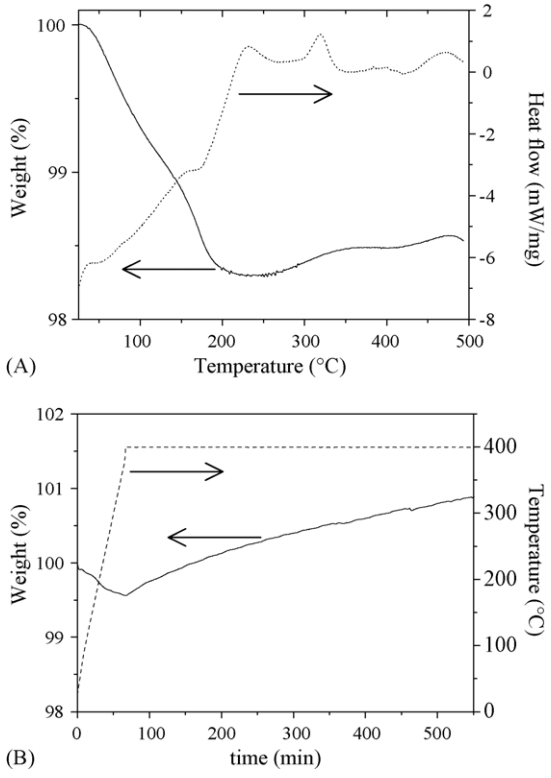

Fig. 1. (A) TGA/DSC curves for the Cu–P foil, straight line corresponds to TGA analysis and the dotted line corresponds to DSC analysis. (B) TGA curve for the Cu–P foil, keeping the temperature at 400 °C for 8 h. Both samples were analysed before any thermal treatment.

A second sample was heat treated at 400 °C for 8 h in the TGA analyser (Fig. 1B). As in the first sample, there was an insignificant weight loss, <1%, between room temperature and 400 °C. After that, when the sample was kept at 400 °C for 8 h, the sample increased its weight only by 1% approximately. This effect might be attributed to oxidation, due to the presence of small quantities of oxygen into the TGA chamber. The XRD analysis of the sample did not show any other compounds, than Cu_3P.

Fig. 2 shows the different XRD patterns obtained for the Cu–P foils without annealing and heat treated between 200 and 400 °C for 8 h. The maximum temperature was 400 °C because phosphorus sublimates at 416 °C in these conditions [19]. The samples without annealing and heat treated at 100 °C only showed the peaks of metallic copper (JCPDS file 85-1326) [20]. Phosphorus was not detected due to its weak diffraction coefficient. Small amounts of Cu_3P could be detected on the sample fired at 200 °C (JCPDS file 71-2261) [21], and XRD patterns of the samples fired at 300 and 400 °C presented the typical diffraction pattern of Cu_3P. At 300 °C, the main phase was Cu_3P and still small quantities of metallic copper were detected from the Cu foil. On the other hand, Cu_3P was the only phase detected by XRD for the sample heat treated at 400 °C. In this study, the XRD analysis did not allow to quantify the volumetric percentages of the compounds produced in the samples due to the lack

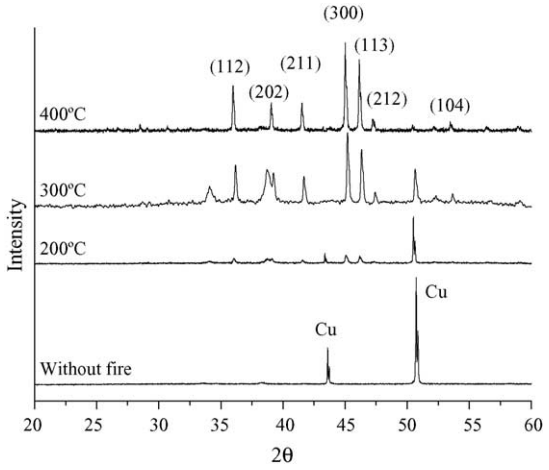

Fig. 2. X-ray diffraction patterns of the Cu–P samples heat treated for 8 h at different temperatures.

of signal for the phosphorus and the excess of copper from the Cu foil. However, it is clear that the synthesis of Cu_3P is strongly favoured at 400 °C.

The synthesis of several metal phosphides has been reported in the literature [6,9–18]. However, all of them are produced at high temperatures. Hence, we attempted the same kind of synthesis used to yield Cu_3P, using foils of several other transition metals. The metals tested were Ti, Cr, Ni, Fe, Mn and Zn, all of them are transition metal of the first series like Cu. Although binary phosphide compounds are reported with all these metals, none of them produced the metal phosphide when the samples were fired under the same conditions as copper (400 °C for 8 h, in flowing Ar). Some of the transition metals produced their corresponding metal phosphide when the samples were fired at higher temperatures, ≥700 °C. However, these experiments had to be done in sealed quartz tubes, due to the sublimation point of phosphorus, 416 °C, and subsequently, these synthesis are far more difficult to scale up for the production of large amount of powder compared to the simple low cost synthesis of Cu_3P.

Copper was the only transition metal of the first series that produced a phosphide at low temperatures by direct reaction between the metal and phosphorus. The enthalpies of formation at 298.15 °C for different metal phosphides have been reported previously and are presented in Table 1; [6]. The

Table 1
Enthalpies of formation of different metal phosphides

Metal phosphide (kJ/mol)	ΔH_f° at 298.15 °C (kJ/mol)
Cr_3P	−163.05
Mn_3P	−179.80
Fe_3P	−142.84
Fe_2P	−130.82
Ni_3P	−187.00
Cu_3P	−166.10
Zn_3P_2	−147.02
ZnP_2	−71.33

Data reproduced from Schlesinger [6].

enthalpy values for the different transition metal phosphides do not show any kind of trend. Furthermore, no values are reported for heat capacities (ΔC_p), or kinetic data like activation energy. These data could help to estimate the enthalpies at the reaction temperatures. For these reasons, it is not easy to explain the observed behaviour. One possible explanation could be that all the elements of the first transition series have partially filled 3d shells, except copper and zinc. Nevertheless, only the copper has a complete 3d shell, and a single 4s electron outside the 3d shell [22]. Then, copper is the only element in the series to have a M^{+1} state. This unique electronic configuration may facilitate the solid-state reaction between copper and phosphorus (reaction (1)). Further and more specific experiments have to be performed to probe completely this hypothesis.

$$3Cu + P \rightarrow Cu_3P \quad (1)$$

3.2. Morphology and surface analysis of the Cu_3P thick films

The morphology of the Cu_3P film produced over the Cu foil at 400 °C is shown in Fig. 3. In general, the Cu_3P films presented an inhomogeneous and porous structure, produced by agglomerates with a particle size ranging between 5 and 40 μm. A closer examination of these agglomerates showed that they were made of tiny particles smaller than 1 μm. The morphology observed, for the Cu_3P thick films, is very convenient and useful to allow the electrolyte impregnation and a good reactivity during the electrochemical test (see Section 3.3).

In order to better understand the formation mechanism and morphology of the Cu_3P films, samples heat treated at 200 and 300 °C were analysed by SEM. The micrographs of these samples are shown in Fig. 4. Sample without any thermal treatment clearly shows how the particles of phosphorus are merely deposited over the Cu foil (Fig. 4A). The size of these grains ranges from 2 to 30 μm. Furthermore, EDS analyses showed the presence of oxygen and carbon in the phosphorus particles. The concentration of these elements detected in the phosphorus particles was up to 15 and 25% of oxygen and carbon, respectively. The presence of these elements must be due to the solvent and water still present in the phosphorus particles. These results are in agreement with the TGA/DSC results.

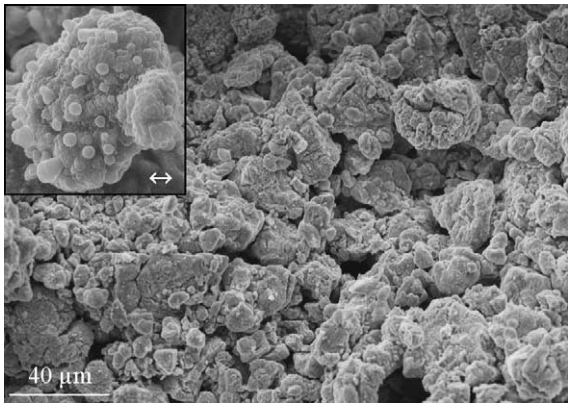

Fig. 3. SEM micrograph of the Cu_3P film produced over the Cu foil at 400 °C for 8 h. The arrow in the small picture corresponds to 1 μm.

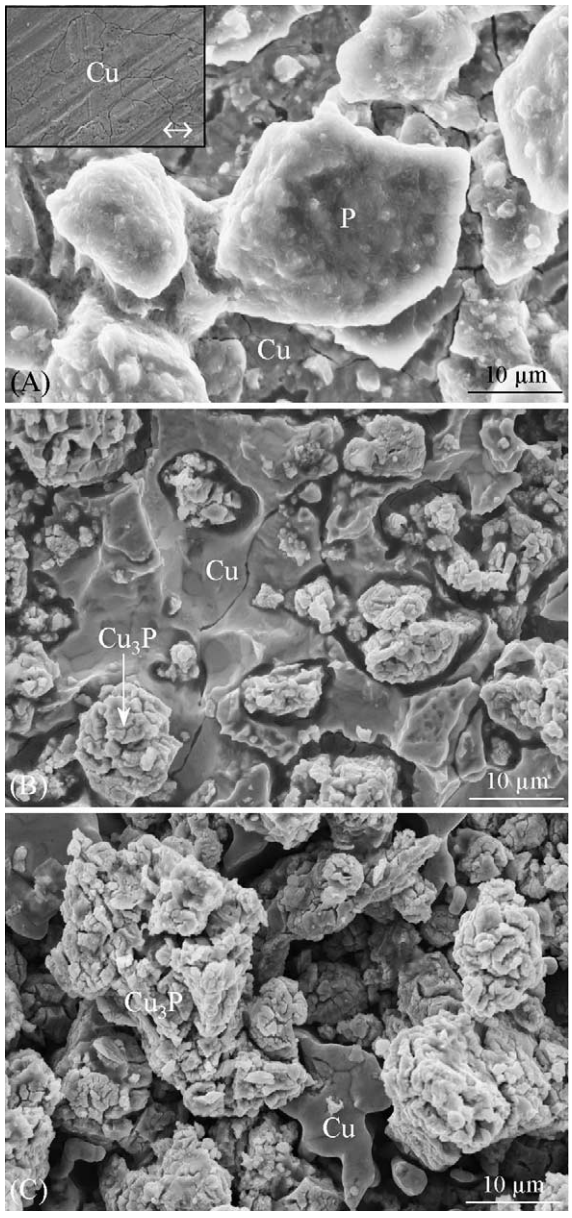

Fig. 4. SEM micrographs of the Cu–P foil before the thermal treatment (A) and the samples heat treated at 200 °C (B) and 300 °C (C) for 8 h. The arrow in the small picture of the Fig. 3A corresponds to 10 μm.

When the sample was fired at 200 °C, the production of Cu_3P was evidenced by XRD (Fig. 2). SEM observations allowed to detect Cu_3P particles over the Cu substrate (Fig. 4B), and these particles seem to dig the copper foil. Apparently, phosphorus is diffusing and reacting into the copper structure. As a consequence, the Cu foil presents holes where the Cu_3P particles are held. The EDS analysis indicated the following composition: P = 23 at.% and Cu = 77 at.%, thus confirm-

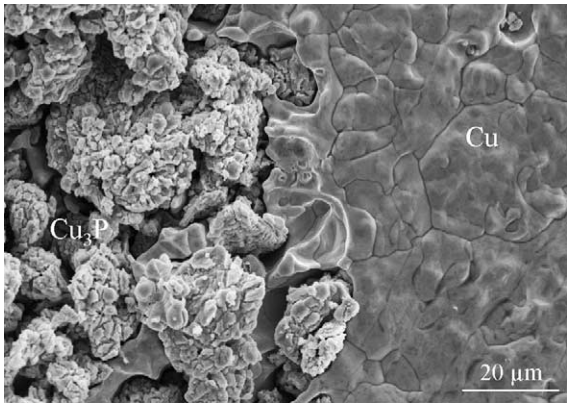

Fig. 5. SEM micrograph of the Cu foil, where just the middle of the foil was sprayed with phosphorus and fired at 400 °C for 8 h.

ing a Cu/P molar ratio close to 3. The sample heat treated at 300 °C presented the same behaviour as the sample annealed at 200 °C. However, in this sample, the population of Cu_3P particles was much higher (Fig. 4C). It is clear that by increasing the temperature, the concentration of Cu_3P increases, covering the Cu foil. To confirm that the change in surface morphology of the Cu foil seen in Figs. 3 and 4 arose from the formation of Cu_3P as a result of the phosphorus diffusion into the copper foil, Fig. 5 shows a sample where only the middle of the Cu foil was sprayed with phosphorus and then fired at 400 °C for 8 h. Indeed, in the area that was spayed with phosphorus, the Cu_3P particles are held into the holes produced on the Cu foil. On the other hand, the area of the Cu foil that was not sprayed did not present any change. This micrograph confirms that phosphorus is diffusing and reacting into the Cu foil, producing these holes in the Cu foil.

Fig. 6 shows the cross section of the Cu_3P–Cu foil. This figure confirms the presence of two different phases in the surface region. The difference in contrast seen in the backscattered electron image (BSEI) of Fig. 6A arises from the differences in the mean atomic number, $\bar{Z}$, of Cu ($\bar{Z} = 29$) and Cu_3P ($\bar{Z} = 25.5$) [23]. Furthermore, EDS analyses were in excellent agreement with the BSEI image. On the other hand, the Cu/P ratio was close to 3 for the darkest phase. This composition agrees with the Cu_3P stoichiometry. On the other hand, the brighter phase almost did not contain any phosphorus, only 3 at.%, meaning that there is just a little amount of phosphorus in the Cu phase, due to the diffusion process. This value is in good agreement with the solubility of phosphorus in copper at 400 °C, which is around 1.5–2.0 at.%. Furthermore, in Fig. 6A, it is possible to see some small Cu particles that were removed and surrounded by Cu_3P, during the synthesis. Finally, the cross section shows an inhomogeneous Cu_3P thick film. The thickness of the Cu_3P ranged from 30 to 100 μm (Fig. 6B). The thickness and depth of the Cu_3P phase, into the Cu foil, must be correlated to the quantity of phosphorus deposited in each part of the Cu surface during the spray process. This suggests a need for a better control of the phosphorus deposition process.

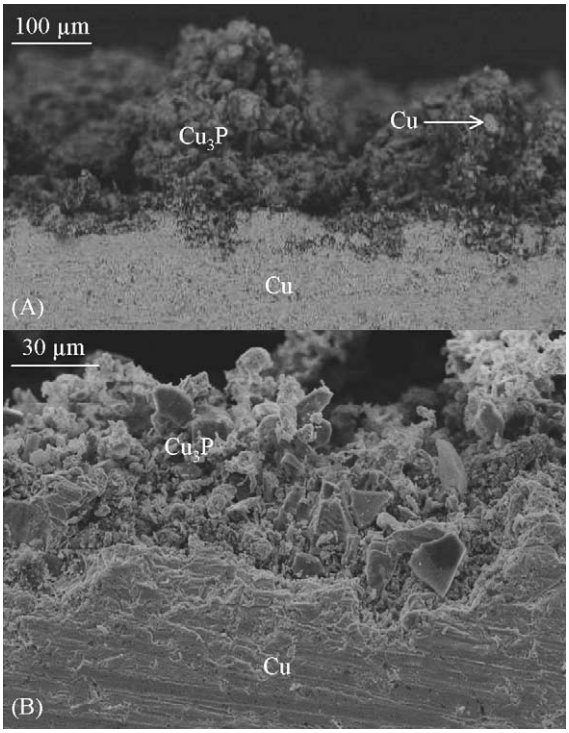

Fig. 6. BSEI (A) and SEI (B) micrographs of the cross section of the Cu_3P–Cu foil heat treated at 400 °C for 8 h. EDS analyses: surface phase Cu = 79 at.% and P = 21 at.%; bulk phase Cu = 97 at.% and P = 3 at.%.

The Cu_3P film was analysed by XPS, where the binding energy bands studied were Cu ($2p_{3/2}$), O (1s) and P (2s). The percentage of the three elements are indicated in Table 2. The presence of oxygen in the sample could be attributed to the formation of a thin oxide layer over the surface of the Cu_3P thick film. A close examination of the XPS spectra in the phosphorus region showed a double peak. The binding energies for these two peaks were 134.6 and 129.5 eV (Fig. 7). The binding energy peak at 134.6 eV corresponds to a P-bonded oxygen, in the form of phosphate [24]. This peak corresponds to the phosphorus present on the oxide surface layer. On the other hand, the second peak appeared at lower binding energies, 129.5 eV. There is not any reference for a P-bonded copper binding energy and there are just a few binding energies reported for P-bonded metallic elements [24]. All of them present lower energies than the red phosphorus at 130.2 eV. Hence, the binding energy band at 129.5 eV should correspond to the P-bonded copper in the Cu_3P.

The presence of an oxidized surface must modified the electrochemical behaviour of the material. Actually, the oxide phase present on the Cu_3P surface produced some irre-

Table 2
XPS elemental percentage analysis

Element	Before ablation	After ablation
Cu	38.4	50.4
P	26.3	28.2
O	35.3	21.4

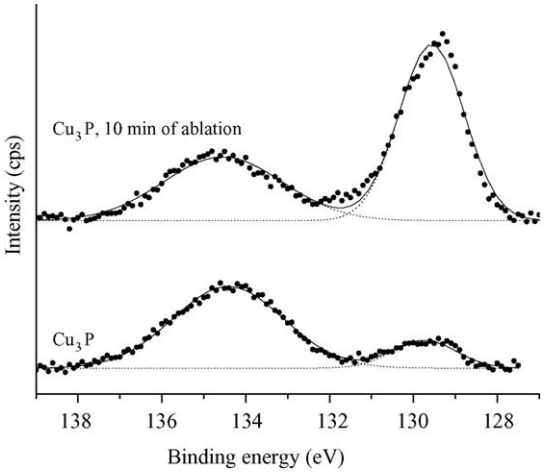

Fig. 7. XPS spectra of the binding energy band (2s) for phosphorus, before and after 10 min of ablation.

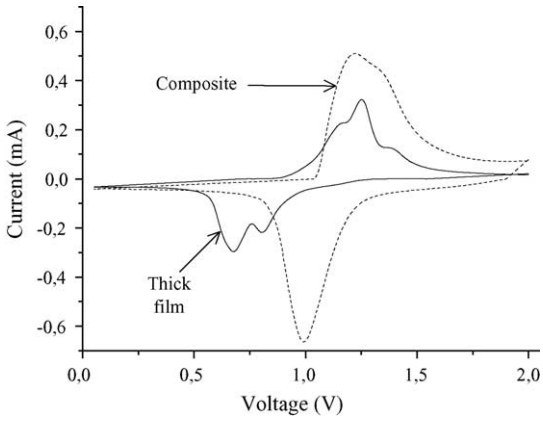

Fig. 8. First cyclic voltamograms of the thick film and composite electrodes of Cu_3P vs. Li at 10 mV/min.

versible capacity during the first cycles of charge/discharge (see Section 3.3).

Finally, as can be seen in Fig. 7, the intensity of the P-bonded oxygen peak decreased as a function of the ablation process. Meanwhile, the intensity of the P-bonded copper peak increased. This change in the concentration of the two different kinds of phosphorus at the surface is in agreement with the proposition of a thin oxide layer on the surface, which is disappearing due to the ablation process. In fact, the oxygen quantity decreased from 35.3 to 21.4 at.% after the ablation process. Furthermore, this agrees with the small increment of the weight observed during the TGA analysis (Fig. 1), where there was an increment of about 2% of the weight, and it was attributed to an oxidation process of the surface. The detection of this oxidized layer is very important, since it may have a huge impact on the electrochemical behaviour of the material.

3.3. Electrochemical comparison between Cu_3P thick films and composite electrodes

Since no Li–Cu binary compounds have been reported in the literature, the reaction in which the maximum lithium uptake is admitted could be:

$$Cu_3P + 3Li \rightarrow 3Cu + Li_3P \quad (2)$$

From this reaction, a reversible capacity of 377 mAh/g or 2778 Ah/L can be envisioned. Practically, reaction (2) does not truly reflect what occurs to Cu_3P upon reduction. Previous studies have shown that several steps are involved with Li_2CuP as an intermediate compound [7,18,25,26], leading to a true displacement reaction, where copper is progressively extruded from the pristine structure and replaced by lithium. The similarities between the different structures encountered upon reduction facilitate to re-incorporation of the copper on the subsequent oxidation. Such a mechanism could be of great interest since it suggests a strong reversibility of reaction (2) and subsequently a high long term cycling ability.

Some electrochemical characterizations of the Cu_3P as anode material for lithium ion batteries have already been reported [7,18,25,26]. However, here is presented a comparison of the electrochemical behaviour between the Cu_3P thick film without any further treatment, and a standard composite electrode. Fig. 8 shows the first voltamograms of the Cu_3P thick film and the Cu_3P composite electrodes, respectively. The composite electrode presents a well defined reduction peak at 1 V versus Li/Li^+. On the other hand, the peak of the thick film, for the same reduction reaction, is shifted toward lower potentials, 0.6 V versus Li/Li^+. The difference between these two reduction peaks must be attributed to the presence of the carbon conductive additive in the composite electrode, which produce a lower polarization of the pristine material. Although the potential, for the reduction reactions, is different for the two electrodes, the oxidation reactions did not present any significant difference. The charge processes were performed between 0.9 and 1.5 V. The same observations are made on the galvanostatic cycles (Fig. 9). Moreover, the open circuit voltage (OCV) of both electrodes lies at around 3.1 V versus Li^+/Li. The galvanostatic plots did not show significant reductions between the OCV and 1.5 V. Afterwards, a pseudo plato, with slight slopes, can be observed at lower voltages than 1.5 V. The pseudo platos, of the thick films at the different rates, were observed at lower voltages than those observed for the composite electrodes. It was already explained by the presence of carbon conductive additive.

The capacities obtained from the galvanostatic measurements at C/20 rate, exceed the theoretical capacity of 363 mAh/g. Both samples, the thick film and the composite electrode, produced capacities higher than 600 mAh/g. Other reported results [7,18,25,26] indicate an excess capacity in comparison with the theoretical value expected for Cu_3P. The same feature has already been observed for oxides such as CuO, where the excess capacity is explained by a combination of lithium insertion and the fact that extra reactions are take place. In the case of Cu_3P, the unoptimised electrolyte

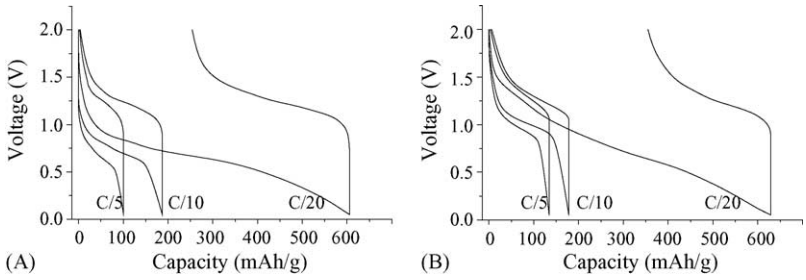

Fig. 9. Galvanostatic cycles of the thick film (A) and composite (B) electrodes of Cu_3P vs. Li at different rates.

should be involved in this reactions, as suggested by Crosnier et al. [25]. Additionally, the presence of oxidized species on the surface of the material was evidenced by XPS analysis. These oxidized compounds could bring some extra capacity during the reduction step. Such capacity would be mostly irreversible.

However, the charge capacities of the first cycles for the thick film and composite were only 360 and 275 mAh/g, respectively. These values are consistent with the involvement of three lithium atoms per Cu_3P, as expected from reaction (2). This corroborates the fact that the electrolyte as well as the oxidized layer are involved in irreversible reactions during the reduction process. Since the capacities of both samples also exceed 377 mAh/g during the second reduction, it is probable that the electrolyte is also consumed during the following cycles (Fig. 10).

Both samples, the thick film and the composite electrodes, present comparable capacity fade upon cycling. After only 10 cycles at C/20 rate a stable capacity around 200 mAh/g seems to be reached (Fig. 10). Thick film sample shows little advantage versus composite electrode. Nevertheless, the composite electrode can stand higher cycling rate with only a small capacity loss than that of the thick film, which exhibits a severe drop in capacity at C/10. At this rate, the composite stabilises at around 200 mAh/g, while the thick film drop down to 150 mAh/g. Finally, at a rate of C/5, the same behaviour is observed. The composite electrode stabilises at higher capacities than the thick film, 150 and 110 mAh/g, respectively. These performances can be attributed to the presence of a binder and a conductive material in the composite electrode. Pfeiffer et al. [7] reported that Cu_3P expands and contracts during the charge/discharge processes. Hence, the presence of these additives optimise the contact of the Cu_3P particles with the current collector, and increased the electronic conductivity, thus leading to an enhanced electrochemical behaviour at fast cycling rates.

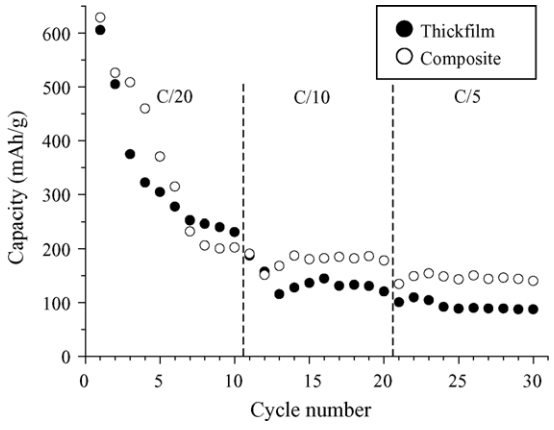

Fig. 10. Capacities as a function of the cyclability for the film and composite electrodes of Cu_3P, at different rates.

4. Conclusions

Cu_3P was prepared by solid-state reaction at low temperature, 400 °C. This new and very simple method of synthesis may allow an industrial production due to its straightforward procedure, in comparison to the normal methods of synthesis reported for metal phosphides so far. The synthesis of others phosphides, using different transition metals of the first series, was unsuccessful using the same low temperature procedure. Although the thermodynamic data reported for these compounds are not sufficient to explain this behaviour, it is possible that the special electronic configuration of copper is causing the differences with the other transition metals of the first series.

Temperature was found to be an important factor in the reaction mechanism of the Cu_3P synthesis. The optimum temperature for the synthesis was 400 °C. According with SEM observations, Cu_3P is produced by phosphorus diffusion into the Cu foil and its subsequent reaction, leading to the formation of agglomerates which are formed by tiny particles of 1 μm diameter approximately. Furthermore, a thin oxidized layer was produced over the surface of the Cu_3P thick film.

Cu_3P thick film and composite electrodes, both present excess capacity during the first reduction step. This can be explained by the fact that extra reactions are taking place, probably involving the electrolyte. Both kinds of samples showed a good cycling behaviour at C/20 rate. The composite electrodes exhibited a better cycling behaviour than that of the thick films at faster cycling rates. However, the electrochemical behaviour of Cu_3P resembles the one of previous alternative materials to graphite, with an interesting first cycle capacity, but a quick fade upon cycling and a high working potential compared with graphite. For these reasons, Cu_3P

cannot compete with graphite in standard lithium ion batteries. However, it may present interest in alternative devices as anode materials for lithium ion batteries, where special issues are required, for example safety.

Acknowledgements

H. Pfeiffer thanks to the Région des Pays de la Loire France, for financial support during his postdoctoral stage at the University of Nantes. The authors would like to thank Dr. O. Crosnier and Dr. V. Fernandez of the Institut des Matériaux Jean Rouxel, for all the facilities during the achievement of the TGA/DSC and XPS analyses.

References

[1] G. Pistoia, Lithium Batteries, New Materials Developments and Perspectives, Industrial Chemistry Library, vol. 5, Elsevier, New York, 1994.
[2] W.A. van Schalkwijk, B. Scrosati, Advances in Lithium Ion Batteries, Kluwer Academic/Plenum Publishers, New York, 2002, p. 11.
[3] J.M. Tarascon, M. Armand, Nature 414 (2001) 359.
[4] R.M. Dell, Solid State Ionics 134 (2000) 139.
[5] C.A. Vincent, Solid State Ionics 134 (2000) 159.
[6] M.E. Schlesinger, Chem. Rev. 102 (2002) 4267.
[7] H. Pfeiffer, F. Tancret, M.P. Bichat, L. Monconduit, F. Favier, T. Brousse, Electrochem. Commun. 6 (2004) 263.
[8] Y.U. Kim, C.K. Lee, H.J. Sohn, T. Kang, J. Electrochem. Soc. 151 (2004) A933.
[9] D.C.S. Souza, V. Pralong, A.J. Jacobson, L.F. Nazar, Science 296 (2002) 2012.
[10] R. Alcántara, J.L. Tirado, J.C. Jumas, L. Monconduit, J. Olivier-Fourcade, J. Power Sources 109 (2002) 308.
[11] V. Pralong, D.C.S. Souza, K.T. Leung, L. Nazar, Electrochem. Commun. 4 (2002) 516.
[12] M.L. Doublet, F. Lemoigno, F. Gillot, L. Monconduit, Chem. Mater. 14 (2002) 4126.
[13] L. Monconduit, F. Gillot, M.L. Doublet, F. Lemoigno, Ionics 9 (2003) 56.
[14] F. Gillot, M.P. Bichat, F. Favier, M. Morcrette, J.M. Tarascon, L. Monconduit, Ionics 9 (2003) 71.
[15] M. Morcrette, F. Gillot, L. Monconduit, J.M. Tarascon, Electrochem. Solid State Lett. 6 (2003) A-59.
[16] D.C.C. Silva, O. Crosnier, G. Ouvrard, J. Greedan, A. Safa-Sefat, L. Nazar, Electrochem. Solid State Lett. 6 (2003) A-162.
[17] K. Wang, J. Yang, J. Xie, B. Wang, Z. Wen, Electrochem. Commun. 5 (2003) 480.
[18] M.P. Bichat, T. Politova, H. Pfeiffer, F. Tancret, L. Monconduit, T. Brousse, F. Favier, J. Power Sources 136 (2004) 80.
[19] R.C. Weast, M.J. Astle, Handbook of Chemistry and Physics, 61st ed., CRC Press Inc., 1981.
[20] H.E. Swanson, E. Tatge, Natl. Bur. Stand. (U.S.) 1 (1953) 539.
[21] O. Olofsson, Acta Chem. Scand. 26 (1972) 2777.
[22] F.A. Cotton, G. Wilkinson, C.A. Murillo, M. Bochmann, Advanced Inorganic Chemistry, John Willey & Sons, New York, 1999, p. 633.
[23] J.I. Goldstein, D.E. Newbury, P. Echlin, D.C. Joy, E. Fiori, Scanning Electron Microscopy and X-ray Microanalysis, Plenum, New York, 1981, p. 75.
[24] D. Briggs, M.P. Seah, Practical Surface Analysis, by Auger and X-ray Photoelectron Spectroscopy, John Wiley & Sons, New York, 1983, p. 484.
[25] O. Crosnier, L. Nazar, Electrochem. Solid State Lett. 7 (2004) 187.
[26] M.P. Bichat, T. Politova, J.L. Pascal, L. Dupont, M. Morcrette, L. Monconduit, F. Favier, J. Electrochem. Soc. 151 (2004) 2074.